channel agonist, (−)-Bay K8644, resulted in significant stimulation of C-peptide release, suggesting the presence of functional K_{ATP} channels (Sturgess et al., 1985) and L-type voltage-dependent Ca^{2+} channels (Misler et al., 1992). The results also showed that increasing the cAMP level by using IBMX resulted in significantly increased C-peptide secretion, indicating the cells' responsiveness to cAMP, which influences insulin secretion (Prentki and Matschinsky, 1987; Pyne and Furman, 2003). Moreover, treatment of the differentiated cells with carbachol (a muscarinic agonist) also significantly increased the secretion of C-peptide. Immunocytochemical analysis also demonstrated that ~50% of all INS- or CP-positive cells co-expressed PDX1, UCN3, IAPP, and ISL1 (Supplementary Figure S3C). Taken together, these results suggest that a fraction of INS-expressing cells derived from this culture system possesses pancreatic β-cell like characteristics.

NOGGIN and IBMX enhanced differentiation into INS single-positive cells

We next examined the key factors that promoted and properly directed hiPS-derived cells to differentiate into INS single-positive cells. We found that the *INS* expression (Figure 6A and B) and proportion of INS-expressing cells (Figure 6C and D) were significantly upregulated only when we added 200 ng/ml of NOGGIN (Nog 200) at stages 3 and 4 and IBMX at stage 5. Importantly, adding both 200 ng/ml of NOGGIN at stages 3 and 4 and IBMX at stage 5 increased the proportion of INS single-positive cells, while it decreased the proportion of poly-hormonal cells. Interestingly, no hormone-positive cells were detected in the absence of NOGGIN, regardless of whether IBMX was used or not. C-peptide content (Figure 6E) and glucose-stimulated C-peptide secretion (Figure 6F) were also significantly increased when IBMX and 200 ng/ml of NOGGIN were used in the differentiation process. The above results support the hypothesis that NOGGIN (at high concentrations) at stages 3 and 4 and IBMX at stage 5 enhanced and controlled the differentiation of hiPS-derived cells into INS single-positive β-like cells.

In vitro-generated INS-expressing cells were free of xenogeneic contamination

Next, we evaluated the degree of non-human-derived contamination by measuring the expression of Neu5Gc. Flow cytometry showed that the expression of Neu5Gc was below the detection limit at stage 4 and at the end of stage 5 when xeno-free culture condition was adopted (Figure 7A–C), indicating that our entire differentiation system is xeno-free. We also examined the pancreatic differentiation of hiPS cells on other commercially available xeno-free scaffolds, e.g. CELLstart (composed of fibronectin) and rhVTN (recombinant human vitronectin), in our xeno-free system. We observed that the cells detached from CELLstart- and rhVTN-coated surfaces and formed large clumps (data not shown). Therefore, CELLstart- and rhVTN-coated surfaces were less suitable than Synthemax-coated surfaces for long-term differentiation culture. Moreover, the differentiation efficiency into pancreatic lineages was better on Synthemax-coated surfaces than on CELLstart- or rhVTN-coated surfaces, as indicated by the significantly higher expression levels of pancreatic marker genes, i.e. *PDX1*, *HNF6*, *NKX6.1*, *HLXB9*, and *INS*, and significantly lower expression levels of hepatic (*AFP*) and intestinal (*CDX2*) marker genes (Figure 7D).

Differentiation of other human ES/iPS cell lines into INS-positive cells

Finally, we examined whether our xeno-free differentiation system could be applied to other human ES/iPS cell lines. We used KhES3, a human ES cell line, and 201B7, a human iPS cell line, and compared their differentiation efficiency into INS-expressing cells to that of Toe (Figure 8A). Quantitative RT–PCR showed that both KhES3- and 201B7-derived cells expressed *INS*, *GCG*, and *SST* transcripts, the extents of which were similar to those of Toe-derived cells (Figure 8B). Immunostaining results showed that both KhES3 and 201B7 cells differentiated into β-like cells (Figure 8C), most of which were INS single-positive like that of Toe-derived cells. We also detected endogenous C-peptide contents in both KhES3- and 201B7-derived cells, the levels of which were similar to that of Toe-derived cells (Figure 8D). In addition, we assessed KhES3- and 201B7-derived cells for their C-peptide secretion in response to high glucose concentration (Figure 8E). Results indicated that C-peptide secretion was significantly increased in both KhES3- and 201B7-derived cells in response to 20 mM glucose (~2.12- and 2.70-fold over basal level, respectively), which were similar to that of the Toe-derived cells (2.55-fold over basal level). These results suggest that our *in vitro* xeno-free system is suitable for pancreatic β-cell differentiation, not only from Toe but also from other human ES/iPS cell lines.

Discussion

In this study, we established a five-step protocol and successfully generated INS-producing β-like cells from hiPS cells *in vitro* that possess endogenous insulin pools and secrete C-peptide in a glucose-sensitive manner. Importantly, we found that optimization of the growth factors is important for directing the differentiation into INS single-positive β-like cells. We applied humanized and/or recombinant factors, chemically defined supplements, and synthetic scaffolds in our *in vitro* culture system. Our protocol is simple, completely xeno-free, and does not include embryoid body formation, cell sorting, or reseeding on other plates.

We found that combined treatment with RA, KAAD-cyclopamine, SB431542, and NOGGIN was effective to induce PP cells at stage 3. Hedgehog signaling has been reported to antagonize RA-mediated specification of pancreatic ECs during zebrafish and mouse embryonic development (Martín et al., 2005; Micallef et al., 2005; Stafford et al., 2006; Tehrani and Lin, 2011). In our differentiation system, the number of AFP-positive cells was lesser at high NOGGIN concentrations (200–300 ng/ml), which is in agreement with previous reports that showed that BMP is required for hepatic differentiation but inhibitory for pancreatic differentiation (Cai et al., 2010; Mfopou et al., 2010). BMP signaling has also been reported to increase CDX2 expression through SMAD4 (Barros et al., 2008), which might explain the downregulation of CDX2 at high NOGGIN concentrations.

At stage 4, we applied a combination of Alk5i, ILV, and NOGGIN and noted the efficient induction of EP cells from PP cells, which

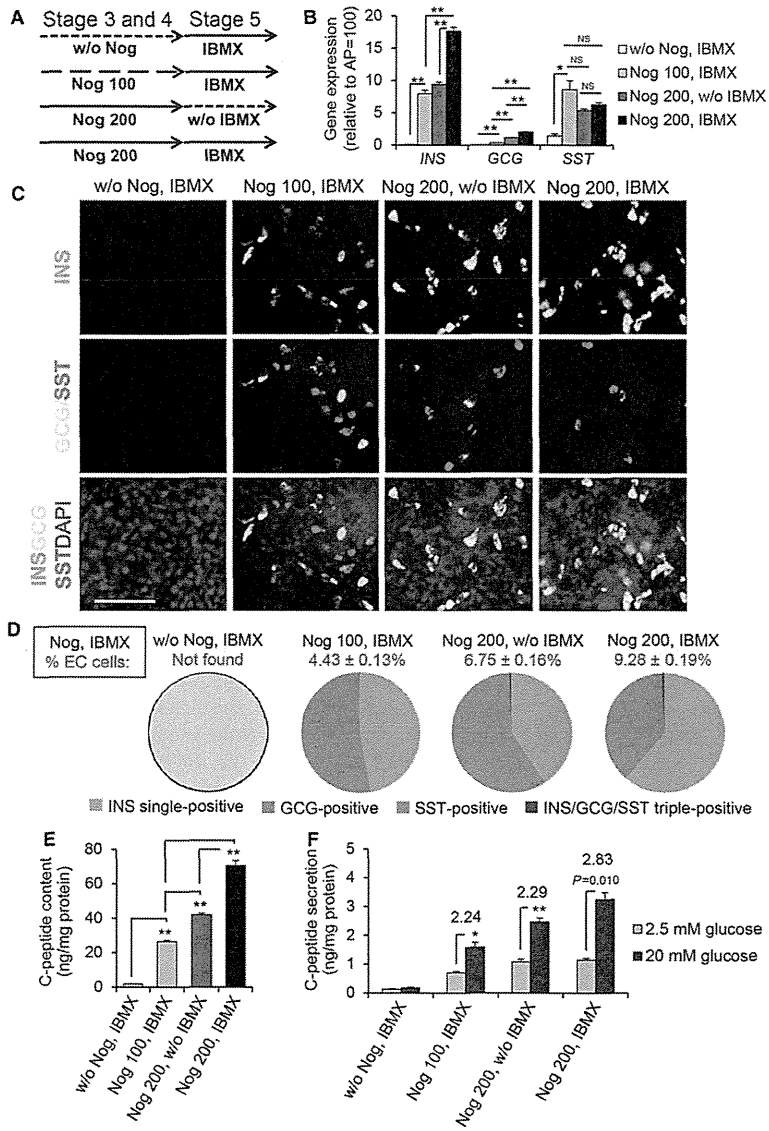

Figure 6 Effect of NOGGIN and IBMX on the generation of INS single-positive β-like cells. INS single-positive cells were derived from PP cells by treatment with Nog 200 and IBMX. (**A**) Schematic drawing of the pancreatic differentiation procedure using various combinations of NOGGIN (*w/o* Nog, Nog 100, and 200 ng/ml with other components at stages 3 and 4) and IBMX (basal medium with or without IBMX at stage 5). (**B**) Relative mRNA expression levels of *INS*, *GCG*, and *SST* in stage-5 cells were determined by quantitative RT–PCR. (**C**) Expression patterns of INS (green), GCG (cyan), and SST (red) in differentiated cells. Cells were counterstained with DAPI (blue). (**D**) Numbers indicate the percentage of pancreatic ECs among all DAPI-positive cells, within which the relative percentages of INS-, GCG-, and SST-positive sub-populations are shown in the pie charts. (**E**) Endogenous C-peptide content in differentiated cells generated at the end of stage 5. (**F**) *In vitro* glucose-stimulated C-peptide secretion of differentiated cells. C-peptide secretion levels under stimulation with 20 mM glucose were compared with those detected under treatment with 2.5 mM glucose. Fold increases are shown on the top of each pair of bars. The *GAPDH* transcript was used as internal RNA control. Expression levels of human adult pancreas genes were calculated and defined as 100. Results are presented as mean ± SEM ($n = 3$). Student's *t*-tests were performed between two discrete data sets for both gene expression and C-peptide level analysis, $*P < 0.05$, $**P < 0.01$. For glucose-stimulated C-peptide secretion, *t*-tests were performed against the values of 2.5 mM glucose treatment, $*P < 0.05$, $**P < 0.01$. AP, adult pancreas. Scale bar, 100 μm.

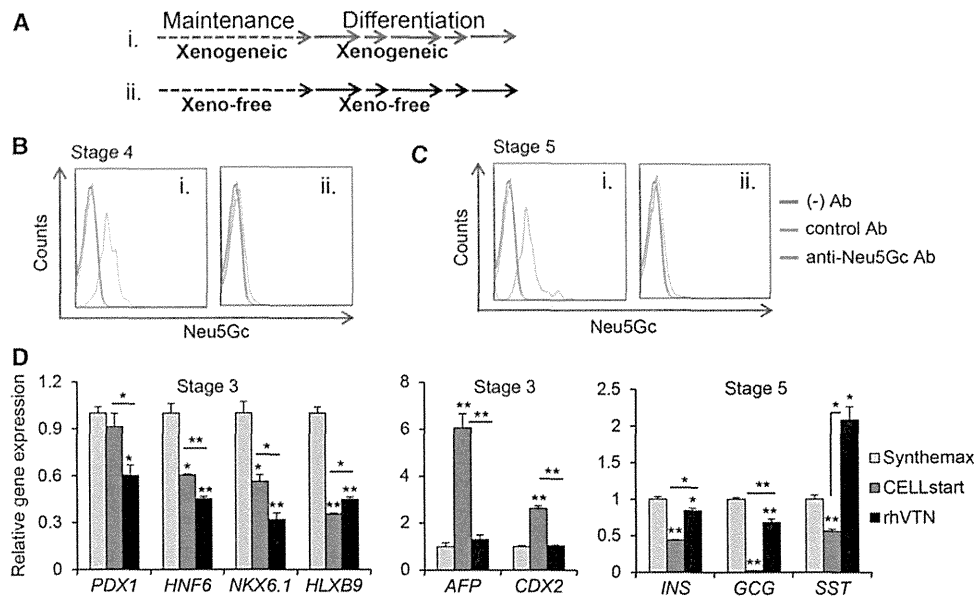

Figure 7 Assay of xenoantigenic contamination in differentiated cell cultures. The entire differentiation system is free of xenogeneic contamination. (**A**) Schematic drawing of the procedures. (**B** and **C**) Detection of Neu5Gc expression in differentiated cells at the end of stage 4 (**B**) and stage 5 (**C**), cultured under xenogeneic (gray bars) or xeno-free (black bars) conditions. Cells were exposed to an anti-Neu5Gc antibody (orange), a negative control antibody (blue), or incubated without primary antibody (red), and then stained with a secondary antibody for analysis. (**D**) Expression levels of pancreatic, hepatic (*AFP*), and intestinal (*CDX2*) marker genes at the end of stages 3 and 5 in cells differentiated under xeno-free conditions using xeno-free scaffolds (Synthemax, CELLstart, and rhVTN). The *GAPDH* transcript was amplified as internal RNA control. Results are presented as mean ± SEM ($n = 3$). Student's *t*-tests were performed against the values of Synthemax or between two discrete data sets. $*P < 0.05$, $**P < 0.01$.

was consistent with recent reports (Rezania et al., 2012, 2013). We successfully induced a high proportion of NGN3-expressing EP cells (Schwitzgebel et al., 2000; Gu et al., 2002), most of which co-expressed NEUROD1 and PAX4. Moreover, the *NGN3* transcript was highly expressed at this stage and gradually disappeared within one or two more days, which is consistent with the transient expression of this gene *in vivo* (Schwitzgebel et al., 2000). *NKX6.1*, an important regulator of the differentiation of pancreatic ECs, in particular, of β-cells (Habener et al., 2005), was expressed in both stage-3 and stage-4 cells, indicating that the progenitor cells derived in our culture system possess the potential to differentiate into pancreatic β-cells.

Nicotinamide is a potent inducer of endocrine differentiation in cultured human fetal pancreatic cells (Otonkoski et al., 1993). In contrast, GLP-1 was reported to increase pancreatic β-cell mass (Buteau et al., 2003). Therefore, we added nicotinamide and exendin-4 (a peptide analog of the GLP-1 receptor) to the final differentiation medium. As expected, CP-expressing β-like cells appeared in the cell culture, however, to a lesser extent. Both IBMX and FRKL in addition to exendin-4 and nicotinamide further promoted differentiation into CP-expressing cells. IBMX and FRKL are known to increase the intracellular cAMP level, suggesting that the cellular cAMP level is one of the key factors that enhance the differentiation of INS-positive cells. Although IBMX and FRKL, in addition to exendin-4 and nicotinamide, similarly promoted the differentiation into CP-positive cells, we considered that the combination of exendin-4, nicotinamide, and IBMX provided a better environment for the induction of EPs to differentiate into INS-expressing cells. This assumption was based on the following observations. First, the number of SST-positive cells was relatively higher in FRKL-induced cells than in IBMX-induced cells, indicating that although both IBMX and FRKL increased the intracellular cAMP level, FRKL might promote SST-positive cells by acting on other pathways. Second, the expression levels of β-cell specific genes were relatively higher in IBMX-induced cells than in FRKL-induced cells.

The differentiated cells obtained in our culture system secreted C-peptide in a glucose-dependent manner; the amount of secreted C-peptide was ~2.8 times higher than the basal level. Previous reports suggested that *in vitro* hES/iPS-derived INS-positive cells have a limited capacity to secrete C-peptide in a glucose-dependent manner (D'Amour et al., 2006; Jiang et al., 2007a, b; Chen et al., 2009; Zhang et al., 2009; Cheng et al., 2012; Kunisada et al., 2012; Bruin et al., 2014). Each report described varying degrees of *in vitro* glucose-stimulated C-peptide secretion, including an ~3-fold increase (Cheng et al., 2012), a 1.7-fold increase (Chen et al., 2009), a 2-fold increase (Jiang et al., 2007b; Zhang et al., 2009), a 3.2-fold increase (Jiang et al., 2007a), and apparently no glucose-stimulated C-peptide secretion (D'Amour et al., 2006; Kunisada et al., 2012; Bruin et al., 2014). These variations

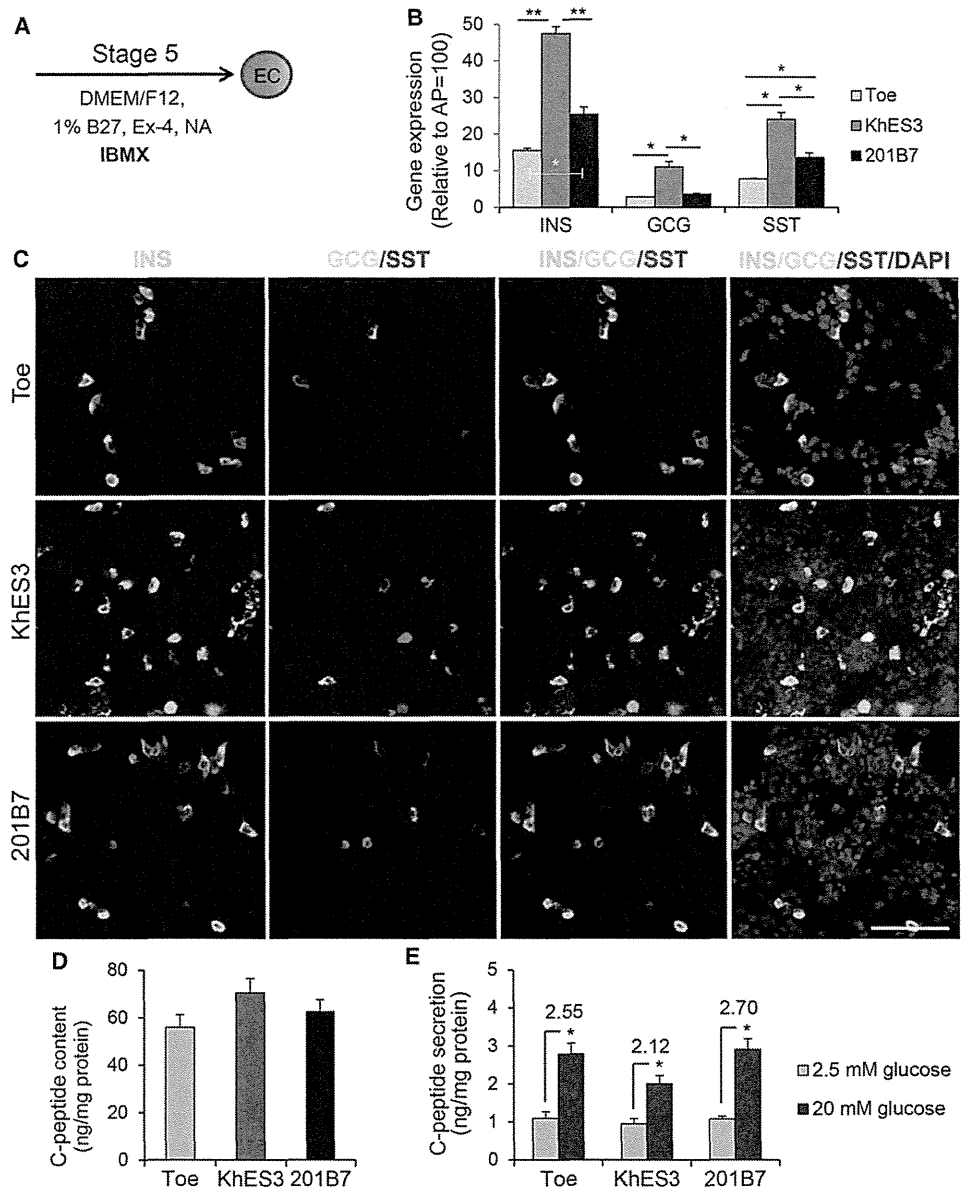

Figure 8 Differentiation of other cell lines into pancreatic ECs. Xeno-free culture system is also suitable for other cell lines for the differentiation into pancreatic β-like cells. Two other cell lines, KhES3 (a hES cell line) and 201B7 (a hiPS cell line) efficiency differentiated into INS single-positive cells, which are similar to that of Toe. (**A**) Factors added to stage-5 basal medium (DMEM/F12, 1% B27, Ex-4, and NA) to promote differentiation into pancreatic ECs were evaluated for the following parameters. (**B**) Relative mRNA expression levels of the endocrine hormones *INS*, *GCG*, and *SST* in cells generated at the end of stage 5 were determined by quantitative RT–PCR. (**C**) Immunocytochemistry showing hormone-positive cells generated at the end of stage 5. INS (green)-, GCG (cyan)-, and SST (red)-positive cells are shown. Cells were counterstained with DAPI (blue). (**D**) C-peptide contents in differentiated cells at the end of stage 5. (**E**) *In vitro* glucose-stimulated C-peptide secretion of differentiated cells at the end of stage 5 was determined by ELISA. C-peptide secretion levels under stimulation with 20 mM glucose were compared with those detected under treatment with 2.5 mM glucose. Fold increases are shown on the top of each pair of bars. The *GAPDH* transcript was used as internal RNA control. Expression levels of human adult pancreas genes were calculated and defined as 100. Results of both quantitative RT–PCR and ELISA are presented as mean ± SEM ($n = 3$). Student's *t*-tests were performed against the values of Toe unless specifically indicated, or between two discrete data sets for both gene expression and C-peptide content analyses, $*P < 0.05$, $**P < 0.01$. For glucose-stimulated C-peptide secretion, *t*-tests were performed against the values of 2.5 mM glucose treatment, $*P < 0.05$, $**P < 0.01$. AP, adult pancreas. Scale bar, 100 μm.

and low levels of secreted C-peptide could be due to the generation of varying numbers of polyhormonal cells in the culture. The existence of polyhormonal cells has been reported during the primary transition stage of early fetal development in humans (De Krijger et al., 1992; Polak et al., 2000). The role and fate of polyhormonal cells during human fetal development are poorly understood; however, immunohistochemical characterization indicated that these cells possess α-cell transcription factor profile (Riedel et al., 2012). Previous studies reported that after transplantation, polyhormonal cells differentiated *in vivo* into GCG-expressing cells, and dynamic chromatin remodeling was reported to occur during this transition into matured cell types (Kelly et al., 2011; Rezania et al., 2011; Basford et al., 2012; Xie et al., 2013). Recently, it has been shown that hES cell-derived pancreatic endoderm cells that were transplanted into immunodeficient mice underwent further differentiation and maturation into glucose-responsive INS-secreting cells (Kroon et al., 2008; Rezania et al., 2012, 2013), suggesting that the pancreatic precursors obtained *in vitro* could mature *in vivo*. Here, in our differentiation culture, addition of IBMX to the culture medium effectively reduced the number of polyhormonal cells and increased the number of INS single-positive cells, which could explain the glucose-stimulated C-peptide secretion *in vitro*. Thus, our results revealed that it is possible to derive INS single-positive β-like cells that have the potential to secrete C-peptide in response to glucose by activating the relevant signaling pathways at the different developmental stages *in vitro*.

Both NOGGIN and IBMX play vital roles in the generation of INS single-positive cells from hiPS-derived cells. We confirmed that the addition of NOGGIN at stages 3 and 4 is indispensable to generate INS-positive cells, regardless of the presence or absence of IBMX, whereas addition of IBMX at stage 5 combined with high doses of NOGGIN (200 ng/ml) at stages 3 and 4 enhanced and regulated the generation of INS single-positive cells. The combined use of high NOGGIN concentrations and IBMX also increased the amount of endogenous C-peptide and glucose-stimulated C-peptide secretion, further supporting the hypothesis that the combined effect of NOGGIN and IBMX is crucial for the generation of INS single-positive β-like cells.

Animal-derived products are undesirable for clinical use. Therefore, in future clinical applications, hiPS cells must be generated, maintained, and differentiated in xeno-free culture systems to minimize the risk. We used xeno-free scaffolds, supplements, and growth factors without any feeder cells, for both maintenance and differentiation. However, to increase the safety of hiPS-based cell therapies, it would be extremely necessary to generate hiPS cells without integrating vectors and continuous c-MYC expression. The generation of hiPS cells with transient expression from non-integrating vectors (Stadtfeld et al., 2008; Yu et al., 2009) may address these concerns.

To our knowledge, this is the first report of a complete xeno-free culture system in which hiPS cells have been differentiated into INS-positive cells. Indeed, our strategy provides evidence towards the possibility of differentiation of hiPS cells into pancreatic β-like cells without contamination by any non-human-derived factors. We believe that our differentiation strategy could be beneficial for the development of future cell therapies. Nevertheless, it also facilitates future *in vitro* studies on the mechanism of human pancreatic specialization and maturation.

Materials and methods

Cell lines

Toe, a hiPS cell line, was established from human embryonic lung cells by infection with retroviruses carrying *OCT4, SOX2, KLF4*, and *C-MYC* genes by Toyoda M., Kiyokawa N., Okita H., Miyagawa Y., Akutsu H., and Umezawa A. (National Institute for Child Health and Development, Tokyo; Yamazoe et al., 2013). We obtained the Toe cell line from the cell bank of the National Institute of Biomedical Innovation, Japan. The cells were initially proliferated and maintained in an undifferentiated state under xenogeneic conditions up to P26 (passage 26) as described previously (Shiraki et al., 2008) and were freeze-stored at −150°C. We also used KhES3, a hES cell line, obtained from Drs Norio Nakatsuji and Hirofumi Suemori (Kyoto University); and 201B7, a hiPS cell line, obtained from Dr Shinya Yamanaka (Kyoto University). Undifferentiated KhES3 and 201B7 were also maintained as described (Shiraki et al., 2008). Human ES cell study was approved by Kumamoto University's Institutional Review Board, following the hES cell guidelines of the Japanese government.

Xenogeneic and xeno-free undifferentiated hES/iPS cell culture

Freeze-stored hES/iPS cells were thawed and cultured on CellBIND cell culture dishes (Corning) coated with a xeno-free synthetic scaffold (Synthemax II-SC Substrate, functionalized with short peptide sequences derived from the vitronectin protein, which is covalently linked to the synthetic acrylate polymer, Corning) under feeder-free conditions with hES/iPS cell maintenance medium.

For xenogeneic culture, the maintenance medium was composed of Knockout DMEM/F12 (Life Technologies) supplemented with penicillin-streptomycin (50 units/ml penicillin, 50 μg/ml streptomycin [PS]; Nacalai Tesque), 2 mM L-glutamine (L-Gln; Nacalai Tesque), 1% nonessential amino acids (NEAA; Life Technologies), 0.1 mM 2-mercaptoethanol (2-ME; Sigma-Aldrich), 20% (*v/v*) knockout serum replacement (KSR; Life Technologies), and 5 ng/ml recombinant human FGF2 (rhFGF2; PeproTech) reconstituted with 0.1% bovine serum albumin (Sigma-Aldrich). Freeze-stored hiPS cells were grown with this maintenance medium for 3–4 days and used for xenogeneic differentiation (Figure 1A).

For xeno-free culture, KSR and rhFGF2 used in the xenogeneic maintenance medium were replaced with the KSR xeno-free Cell Therapy System (CTS; Life Technologies) and rhFGF2 reconstituted with 0.1% recombinant human albumin (Sigma-Aldrich), respectively. The medium was also supplemented with 1% KSR growth factor cocktail CTS (Life Technologies). Xeno-free maintenance medium is, therefore, free from animal-derived factors; rather, it contains all humanized and/or recombinant supplements and defined growth factors. Freeze-stored hES/iPS cells were first grown with xenogeneic maintenance medium for 3–4 days, and then sequentially passaged with xeno-free maintenance medium at a ratio of 1:3 every 3–4 days by dissociating cell colonies with

a cell dissociation buffer (Life Technologies) before they were used for xeno-free differentiation (Figure 1A).

In vitro differentiation of undifferentiated hES/iPS cells

For pancreatic differentiation, undifferentiated hES/iPS cells were dissociated with TrypLE Select CTS (Life Technologies) after three consecutive passages under xeno-free conditions, seeded at a density of 1×10^5 cells/well on 96-well CellBIND cell culture plates coated with Synthemax II-SC Substrate. They were cultured for 1 day using xeno-free maintenance medium containing 10 μM ROCK inhibitor (Y-27632; Wako), followed by another 1–2 days of culture without ROCK inhibitor to 80%–90% confluence. Cells were directed through the following key stages of pancreatic development: DE cells (stage 1), PG cells (stage 2), PP cells (stage 3), EP cells (stage 4), and hormone-expressing ECs (stage 5) (Figure 2A).

At stage 1, cells were cultured for 2 days in DMEM-high glucose (Life Technologies) supplemented with PS, 2 mM L-Gln, 1% NEAA, 0.1 mM 2-ME, 2% (*v/v*) B27 supplement xeno-free CTS (Life Technologies), 100 ng/ml recombinant human activin A (HumanZyme), and 3 μM CHIR99021 (TOCRIS Bioscience), and subsequently for another 3 days cultured without CHIR99021.

At stage 2, cells were cultured for 2 days in RPMI 1640 (Life Technologies) supplemented with PS, L-Gln, NEAA, 2-ME, B27 supplement xeno-free CTS, 0.25 μM KAAD-cyclopamine (Stemgent), and 50 ng/ml recombinant human FGF10 (PeproTech).

At stage 3, cells were cultured for 6 days in DMEM-high glucose supplemented with PS, L-Gln, NEAA, 2-ME, B27 supplement xeno-free CTS, 2 μM all-trans RA (Stemgent), 0.25 μM Cyc, 10 μM SB431542 (CALBIOCHEM), and 200 ng/ml recombinant human NOGGIN (R&D Systems), with the media changed every 2 days.

At stage 4, cells were cultured for 2 days in DMEM-high glucose supplemented with PS, L-Gln, NEAA, 2-ME, B27 supplement xeno-free CTS, 5 μM Alk5i (CALBIOCHEM), 300 nM (−) indolactam V (R&D Systems), and 200 ng/ml NOGGIN.

At stage 5, cells were cultured for 8 days in DMEM/F12 (Cell Science & Technology Inst.) supplemented with PS, L-Gln, NEAA, 2-ME, and B27 supplement xeno-free CTS. To this medium were added 50 ng/ml exendin-4 (Cell Sciences), 10 mM nicotinamide (Sigma-Aldrich), and/or 100 μM IBMX (Wako), and/or 10 μM FRKL (Wako). The media were changed every 2 days.

All factors were reconstituted using 0.1% recombinant human albumin, phosphate-buffered saline (PBS), or DMSO for xeno-free differentiation. A similar xeno-free technique for maintenance and differentiation of hiPS cells was used with the two other xeno-free scaffolds, CELLstart (Life Technologies) and rhVTN (Life Technologies), to compare the differentiation efficiency with that achieved with the Synthemax II SC substrate.

Flow cytometry

Flow cytometry was performed for the xenoantigenic factor Neu5Gc, as described previously (Martin et al., 2005). Briefly, 1.0×10^6 cells in a total volume of 50 μl were incubated at 4°C for 60 min with a chicken anti-Neu5Gc IgY antibody (Ab) (1:200 dilution, Sialix), chicken IgY negative control (1:200 dilution, Sialix), or without a primary antibody. After three washes, cells were incubated at 4°C for 60 min with an Alexa Fluor 488-conjugated donkey anti-chicken antibody (1:500, Molecular Probes). Flow cytometry was performed on a BD FACSCanto Flow Cytometer (BD Biosciences) and analyzed using the FlowJo software (Tree Star, Inc.).

Quantitative RT–PCR analysis

Total RNA was extracted from cells using TRIzol and genomic DNA contamination was removed by digestion with deoxyribonuclease I (Sigma-Aldrich). Total adult human pancreas RNA was purchased from Clontech. cDNA was prepared from 2.0 μg of RNA with oligo-dT primers and the ReverTraAce RT-reagent kit (TOYOBO). The primer sequences used for quantitative RT–PCR are summarized in Supplementary Table S1. Quantitative RT–PCR was carried out on a 7500 FAST Real-Time PCR System (Applied Biosystems) using the Thunderbird Sybr qPCR Mix (TOYOBO). The expression of each target gene was normalized to the expression level of the housekeeping gene glyceraldehyde-3-phosphate dehydrogenase (GAPDH).

Alkaline phosphatase staining

The cultured cells were fixed with 4% (*w/v*) paraformaldehyde (Nacalai Tesque), washed with PBS and then incubated with alkaline phosphatase buffer (100 mM Tris–HCl [pH 9.5], 100 mM NaCl, 50 mM $MgCl_2$, and 0.1% Tween-20) for 30 min at room temperature. The staining reaction was carried out with 4-nitroblue tetrazolium chloride (35 μg/ml) and 5-bromo-4-chloro-3-indolyl phosphate (17.5 μg/ml) (Roche Diagnostics) in the dark for 30 min at room temperature. Cells were then washed with 1 mM EDTA/PBS, fixed with 4% paraformaldehyde, and images were captured.

Immunocytochemistry

Immunostaining was performed as described previously (Yamazoe et al., 2013). Details on the primary antibodies are provided in Supplementary Table S2. The secondary antibodies used were Alexa Fluor 488-, 568-, or 633-conjugated donkey or goat anti-mouse, anti-goat, anti-rabbit, anti-sheep, or anti-guinea pig IgG (1:1000 dilutions; Molecular Probes). Nuclei were counterstained with 4′,6-diamidino-2-phenylindole (DAPI, Roche Applied Science). Images were captured using an ImageXpress Micro scanning system (Molecular Devices, Japan), and quantitative analysis was performed using the MetaXpress cellular image analysis software (Molecular Devices).

C-peptide release and content assay

The C-peptide release and content assay was performed as described previously (Sakano et al., 2014) with minor modifications. Briefly, differentiated cells at the end of stage 5 were pre-incubated at 37°C for 30 min with DMEM (Life Technologies) containing minimal essential medium, 1% B27 supplement, and 2.5 mM glucose. Cells were washed twice with PBS and then incubated at 37°C for 1 h with DMEM containing 2.5 mM glucose at 100 μl per well. The culture medium was collected, and the same cells were further incubated with DMEM containing 20 mM glucose or DMEM containing 2.5 mM glucose supplemented with various stimulants, i.e. 2 μM (−)-Bay K8644 (Sigma-Aldrich), 100 μM tolbutamide (Wako), 250 μM carbachol (Sigma-Aldrich), 0.5 mM IBMX, or 30 mM

potassium chloride (KCl) (Wako), at 37°C for another 1 h. The culture media were collected and stored at −20°C until analysis. Next, the cells were lysed with lysis buffer (0.1% Triton X-100 in PBS) supplemented with 1% protease inhibitor cocktail (Nacalai Tesque). C-peptide secretion into the culture media and C-peptide content of the cell lysates were measured using the human C-peptide ELISA Kit (ALPCO Diagnostics). The amount of C-peptide was normalized to the amount of total protein in the corresponding cell lysate.

Statistical analyses

Data are expressed as mean ± SEM (standard error of the mean). For comparisons of discrete data sets, unpaired Student's *t*-tests were performed. Significance levels or *P*-values are indicated in the figure legends.

Supplementary material

Supplementary material is available at *Journal of Molecular Cell Biology* online.

Acknowledgements

We thank Drs Toyoda M., Kiyokawa N., Okita H., Miyagawa Y., Akutsu H., and Umezawa A. (National Institute for Child Health and Development, Tokyo, Japan), and members of the National Institute of Biomedical Innovation (NIBIO), Japan for providing Toe hiPS cell line. We also thank Drs Norio Nakatsuji and Hirofumi Suemori (Kyoto University) for providing khES3 cell line and Dr Shinya Yamanaka (Kyoto University) for providing 201B7 cell line.

Funding

This work was supported by the 'Funding Program for Next Generation World-Leading Researchers' (LS099 to S.K.), in part by the Global-COE programs ('Cell Fate Regulation Research and Education Unit' to S.K.), the Program for Leading Graduate Schools 'HIGO' (awarded to S.K.), and Grants-in-Aid (26253059 to S.K., 26461638 to N.S. and 26461036 to D.S.) from the Ministry of Education, Culture, Sports, Science and Technology (MEXT), Japan. S.O. is a research fellow of Japan Society for the Promotion of Science.

Conflict of interest: none declared.

References

Barros, R., Pereira, B., Duluc, I., et al. (2008). Key elements of the BMP/SMAD pathway co-localize with CDX2 in intestinal metaplasia and regulate CDX2 expression in human gastric cell lines. J. Pathol. *215*, 411–420.

Basford, L., Prentice, K.J., Hardy, A.B., et al. (2012). The functional and molecular characterization of human embryonic stem cell-derived insulin-positive cells compared with adult pancreatic beta cells. Diabetologia *55*, 358–371.

Bruin, J.E., Erener, S., Vela, J., et al. (2014). Characterization of polyhormonal insulin-producing cells derived in vitro from human embryonic stem cells. Stem Cell Res. *12*, 194–208.

Buteau, J., Foisy, S., Joly, E., et al. (2003). Glucagon-like peptide-1 induces pancreatic beta cell proliferation via transactivation of the epidermal growth factor receptor. Diabetes *52*, 124–132.

Cai, J., Yu, C., Liu, Y., et al. (2010). Generation of homogeneous PDX1^{+} pancreatic progenitors from human ES cell-derived endoderm cells. J. Mol. Cell Biol. *2*, 50–60.

Chen, S., Borowiak, M., Fox, J.L., et al. (2009). A small molecule that directs differentiation of human ESCs into the pancreatic lineage. Nat. Chem. Biol. *5*, 258–265.

Cheng, X., Ying, L., Lu, L., et al. (2012). Self-renewing endodermal progenitor lines generated from human pluripotent stem cells. Cell Stem Cell *10*, 371–384.

Cobo, F., Stacey, G., Hunt, C., et al. (2005). Microbiological control in stem cell banks: approaches to standardisation. Appl. Microbiol. Biotechnol. *68*, 456–466.

D'Amour, K.A., Bang, A.G., Eliazer, S., et al. (2006). Production of pancreatic hormone-expressing endocrine cells from human embryonic stem cells. Nat. Biotechnol. *24*, 1392–1401.

De Krijger, R.R., Aanstoot, H.J., Kranenburg, G., et al. (1992). The midgestational human fetal pancreas contains cells coexpressing islet hormones. Dev. Biol. *153*, 368–375.

Gu, G., Dubauskaite, J., and Melton, D.A. (2002). Direct evidence for the pancreatic lineage: NGN3^{+} cells are islet progenitors and are distinct from duct progenitors. Development *129*, 2447–2457.

Habener, J.F., Kemp, D.M., and Thomas, M.K. (2005). Minireview: transcriptional regulation in pancreatic development. Endocrinology *146*, 1025–1034.

Hansson, M., Tonning, A., Frandsen, U., et al. (2004). Artifactual insulin release from differentiated embryonic stem cells. Diabetes *53*, 2603–2609.

Jacquemin, P., Lemaigre, F.P., and Rousseau, G.G. (2003). The Onecut transcription factor HNF-6 (OC-1) is required for timely specification of the pancreas and acts upstream of Pdx-1 in the specification cascade. Dev. Biol. *258*, 105–116.

Jiang, J., Au, M., Lu, K., et al. (2007a). Generation of insulin-producing islet-like clusters from human embryonic stem cells. Stem Cells *25*, 1940–1953.

Jiang, W., Shi, Y., Zhao, D., et al. (2007b). In vitro derivation of functional insulin-producing cells from human embryonic stem cells. Cell Res. *17*, 333–344.

Kelly, O.G., Chan, M.Y., Martinson, L.A., et al. (2011). Cell-surface markers for the isolation of pancreatic cell types derived from human embryonic stem cells. Nat. Biotechnol. *29*, 750–756.

Kroon, E., Martinson, L.A., Kadoya, K., et al. (2008). Pancreatic endoderm derived from human embryonic stem cells generates glucose-responsive insulin-secreting cells in vivo. Nat. Biotechnol. *26*, 443–452.

Kunisada, Y., Tsubooka-Yamazoe, N., Shoji, M., et al. (2012). Small molecules induce efficient differentiation into insulin-producing cells from human induced pluripotent stem cells. Stem Cell Res. *8*, 274–284.

Li, H., Arber, S., Jessell, T.M., et al. (1999). Selective agenesis of the dorsal pancreas in mice lacking homeobox gene Hlxb9. Nat. Genet. *23*, 67–70.

Martin, M.J., Muotri, A., Gage, F., et al. (2005). Human embryonic stem cells express an immunogenic nonhuman sialic acid. Nat. Med. *11*, 228–232.

Martín, M., Gallego-Llamas, J., Ribes, V., et al. (2005). Dorsal pancreas agenesis in retinoic acid-deficient Raldh2 mutant mice. Dev. Biol. *284*, 399–411.

Mfopou, J.K., Chen, B., Mateizel, I., et al. (2010). Noggin, retinoids, and fibroblast growth factor regulate hepatic or pancreatic fate of human embryonic stem cells. Gastroenterology *138*, 2233–2245.

Micallef, S.J., Janes, M.E., Knezevic, K., et al. (2005). Retinoic acid induces Pdx1-positive endoderm in differentiating mouse embryonic stem cells. Diabetes *54*, 301–305.

Micallef, S.J., Li, X., Schiesser, J.V., et al. (2012). INS$^{GFP/w}$ human embryonic stem cells facilitate isolation of in vitro derived insulin-producing cells. Diabetologia *55*, 694–706.

Misler, S., Barnett, D.W., Pressel, D.M., et al. (1992). Stimulus-secretion coupling in beta-cells of transplantable human islets of Langerhans. Evidence for a critical role for Ca^{2+} entry. Diabetes *41*, 662–670.

Otonkoski, T., Beattie, G.M., Mally, M.I., et al. (1993). Nicotinamide is a potent inducer of endocrine differentiation in cultured human fetal pancreatic cells. J. Clin. Invest. *92*, 1459–1466.

Polak, M., Bouchareb-Banaei, L., Scharfmann, R., et al. (2000). Early pattern of differentiation in the human pancreas. Diabetes *49*, 225–232.

Prentki, M., and Matschinsky, F.M. (1987). Ca^{2+}, cAMP, and phospholipid-derived messengers in coupling mechanisms of insulin secretion. Physiol. Rev. *67*, 1185–1248.

Pyne, N.J., and Furman, B.L. (2003). Cyclic nucleotide phosphodiesterases in pancreatic islets. Diabetologia *46*, 1179–1189.

Rajagopal, J., Anderson, W.J., Kume, S., et al. (2003). Insulin staining of ES cell progeny from insulin uptake. Science *299*, 363.

Rezania, A., Riedel, M.J., Wideman, R.D., et al. (2011). Production of functional glucagon-secreting alpha-cells from human embryonic stem cells. Diabetes *60*, 239–247.

Rezania, A., Bruin, J.E., Riedel, M.J., et al. (2012). Maturation of human embryonic stem cell-derived pancreatic progenitors into functional islets capable of treating pre-existing diabetes in mice. Diabetes *61*, 2016–2029.

Rezania, A., Bruin, J.E., Xu, J., et al. (2013). Enrichment of human embryonic stem cell-derived NKX6.1-expressing pancreatic progenitor cells accelerates the maturation of insulin-secreting cells in vivo. Stem Cells *31*, 2432–2442.

Riedel, M.J., Asadi, A., Wang, R., et al. (2012). Immunohistochemical characterisation of cells co-producing insulin and glucagon in the developing human pancreas. Diabetologia *55*, 372–381.

Sakano, D., Shiraki, N., Kikawa, K., et al. (2014). VMAT2 identified as a regulator of late-stage β-cell differentiation. Nat. Chem. Biol. *10*, 141–148.

Schulz, T.C., Young, H.Y., Agulnick, A.D., et al. (2012). A scalable system for production of functional pancreatic progenitors from human embryonic stem cells. PLoS One *7*, e37004.

Schwitzgebel, V.M., Scheel, D.W., Conners, J.R., et al. (2000). Expression of neurogenin3 reveals an islet cell precursor population in the pancreas. Development *127*, 3533–3542.

Shapiro, A.M. (2011). State of the art of clinical islet transplantation and novel protocols of immunosuppression. Curr. Diab. Rep. *11*, 345–354.

Shapiro, A.M., Ricordi, D., Hering, B.J., et al. (2006). International trial of the Edmonton protocol for islet transplantation. N. Engl. J. Med. *355*, 1318–1330.

Shiraki, N., Yoshida, T., Araki, K., et al. (2008). Guided differentiation of embryonic stem cells into Pdx1-expressing regional-specific definitive endoderm. Stem Cells *26*, 874–885.

Sipione, S., Eshpeter, A., Lyon, J.G., et al. (2004). Insulin expressing cells from differentiated embryonic stem cells are not beta cells. Diabetologia *47*, 499–508.

Skottman, H., and Hovatta, O. (2006). Culture conditions for human embryonic stem cells. Reproduction *132*, 691–698.

Stadtfeld, M., Nagaya, M., Utikal, J., et al. (2008). Induced pluripotent stem cells generated without viral integration. Science *322*, 945–949.

Stafford, D., White, R.J., Kinkel, M.D., et al. (2006). Retinoids signal directly to zebrafish endoderm to specify insulin-expressing β-cells. Development *133*, 949–956.

Sturgess, N.C., Ashford, M.L., Cook, D.L., et al. (1985). The sulphonylurea receptor may be an ATP-sensitive potassium channel. Lancet *2*, 474–475.

Takahashi, K., Tanabe, K., Ohnuki, M., et al. (2007). Induction of pluripotent stem cells from adult human fibroblasts by defined factors. Cell *131*, 861–872.

Tehrani, Z., and Lin, S. (2011). Antagonistic interactions of hedgehog, Bmp and retinoic acid signals control zebrafish endocrine pancreas development. Development *138*, 631–640.

Thomson, J.A., Itskovitz-Eldor, J., Shapiro, S.S., et al. (1998). Embryonic stem cell lines derived from human blastocysts. Science *282*, 1145–1147.

Xie, R., Everett, L.J., Lim, H.-W., et al. (2013). Dynamic chromatin remodeling mediated by polycomb proteins orchestrates pancreatic differentiation of human embryonic stem cells. Cell Stem Cell *12*, 224–237.

Yamazoe, T., Shiraki, N., Toyoda, M., et al. (2013). A synthetic nanofibrillar matrix promotes in vitro hepatic differentiation of embryonic stem cells and induced pluripotent stem cells. J. Cell Sci. *126*, 5391–5399.

Yu, J., Hu, K., Smuga-Otto, K., et al. (2009). Human induced pluripotent stem cells free of vector and transgene sequences. Science *324*, 797–801.

Zhang, D., Jiang, W., Liu, M., et al. (2009). Highly efficient differentiation of human ES cells and iPS cells into mature pancreatic insulin-producing cells. Cell Res. *19*, 429–438.

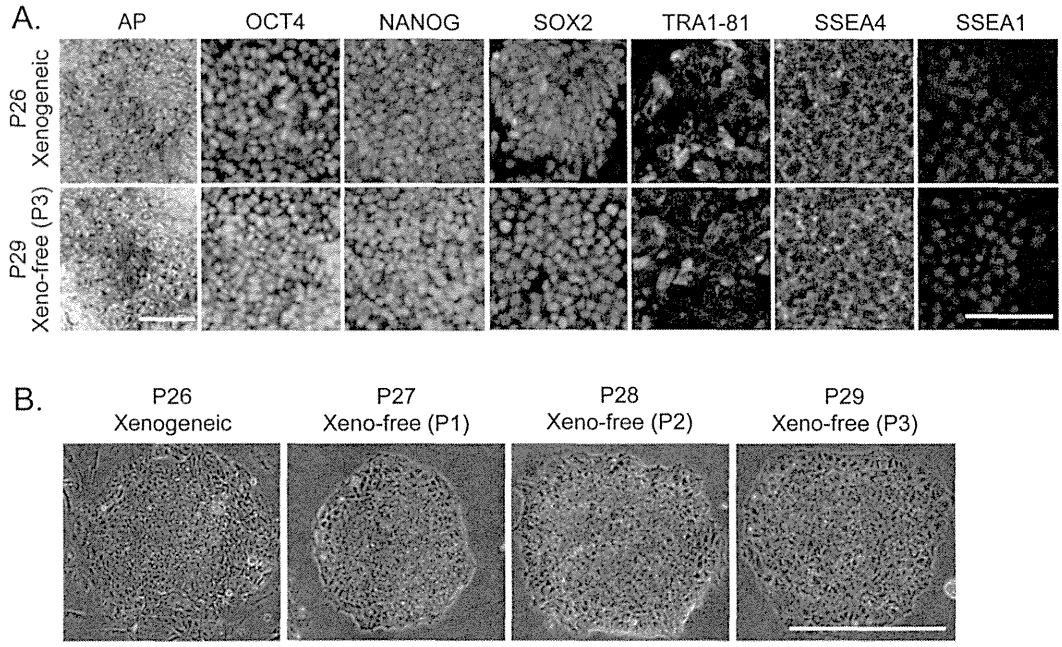

Supplementary Figure S1. Self-renewal and pluripotency of undifferentiated hiPS cells grown under xeno-free conditions

HiPS cells grown under xeno-free conditions showed pluripotent characteristics. A) Undifferentiated hiPS cells grown under xenogeneic and xeno-free conditions were subjected to alkaline phosphatase (AP) staining and immunostaining to compare the expression levels of pluripotency-associated markers. Under both xenogeneic and xeno-free conditions, hiPS cells exhibited a similar expression pattern of pluripotency markers, including OCT4, NANOG, SOX2, TRA-1-81, and SSEA4, confirming adaptation and maintenance of pluripotency under xeno-free conditions. SSEA1-positive cells were not observed among the colonies confirming the undifferentiated state of the cells. B) Bright-field images showing the morphology of hiPS cell colonies grown under xeno-free conditions. Cell nuclei were counterstained with DAPI. P, passage; Scale bars are 100 μm (A) or 1 mm (B).

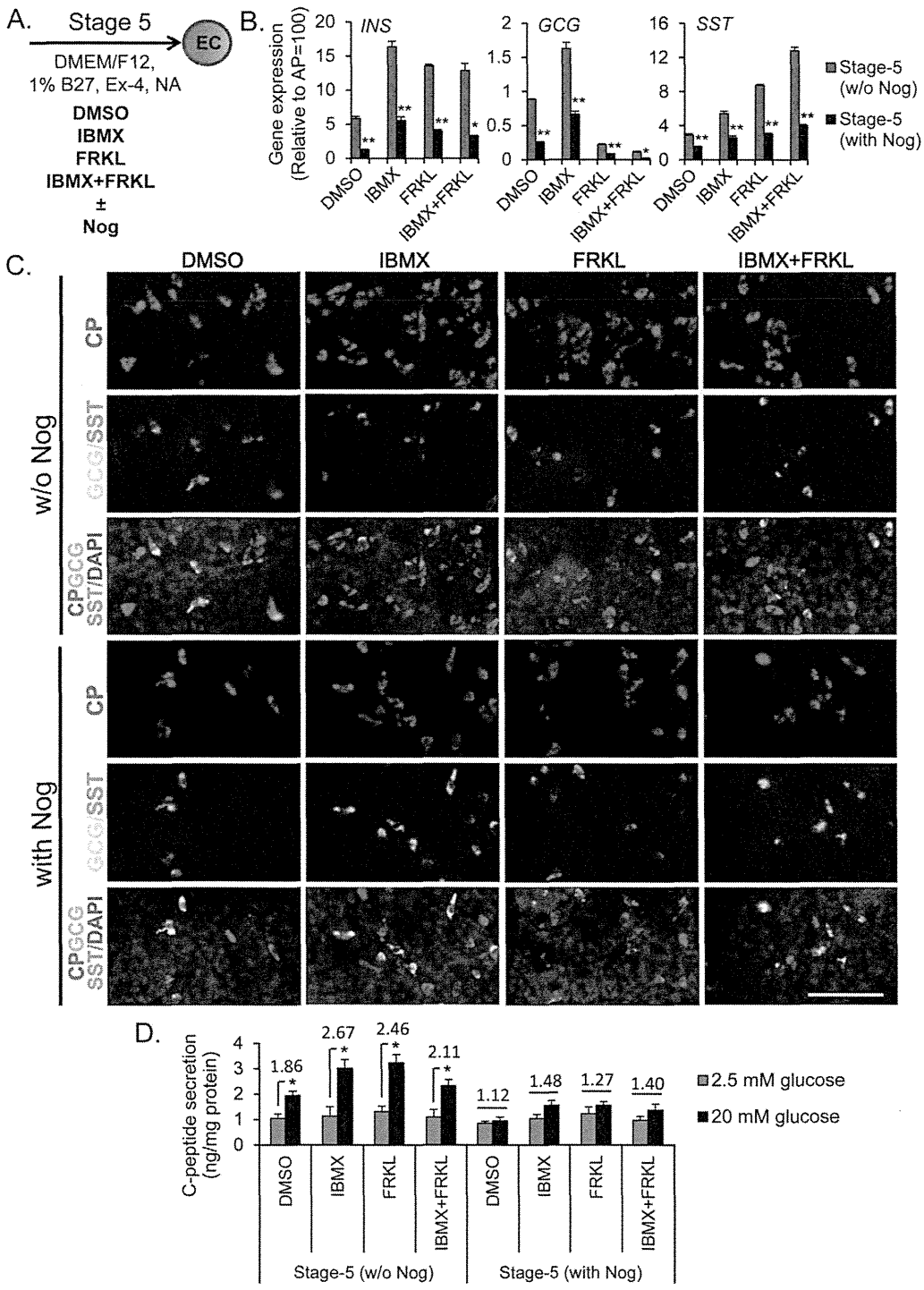

Supplementary Figure S2. NOGGIN at stage-5 culture media reduces the differentiation efficiency into pancreatic endocrine cells (ECs)

Addition of NOGGIN (Nog) to stage-5 culture media reduced the differentiation efficiency into pancreatic β-like cells. A) Nog added to stage-5 culture media to induce differentiation into pancreatic endocrine cells (ECs) was evaluated for the following parameters. B) Relative mRNA expression levels of the endocrine hormones *INS*, *GCG*, and *SST* in cells generated at the end of stage 5 were determined by quantitative RT-PCR. C) Immunocytochemistry showing hormone-positive cells generated at the end of stage 5 in absence or presence of Nog. C-peptide (CP, red)-, GCG (cyan)-, and SST (green)-positive cells are shown. Cells were counterstained with DAPI (blue). D) In vitro glucose-stimulated C-peptide secretion of differentiated cells at the end of stage 5 was determined by ELISA. C-peptide secretion levels under stimulation with 20 mM glucose were compared with those detected under treatment with 2.5 mM glucose. Fold increases are shown on the top of each pair of bars. The *GAPDH* transcript was used as internal RNA control. Expression levels of human adult pancreas genes were calculated and defined as 100. Results of both quantitative RT-PCR and ELISA are presented as mean ± SEM (n = 3). Student's *t*-tests were performed against the values of cells-derived in absence of Nog at stage-5 unless specifically indicated for gene expression, $^{*}p < 0.05$, $^{**}p < 0.01$. For glucose-stimulated C-peptide secretion, *t*-tests were performed against the values of 2.5 mM glucose treatment, $^{*}p < 0.05$, $^{**}p < 0.01$. AP, adult pancreas. Scale bar = 100 μm.

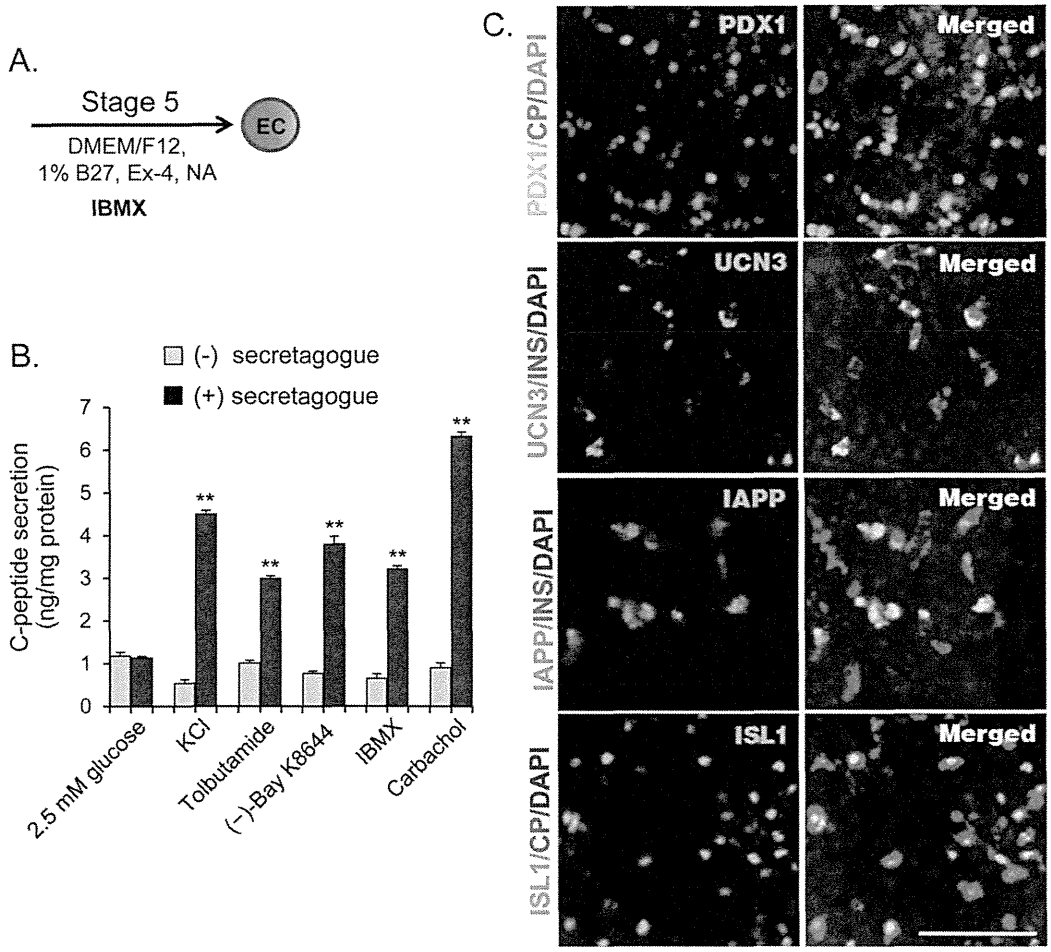

Supplementary Figure S3. Characterization of hiPS cell-derived INS-positive cells

HiPS cell-derived INS-positive cells secreted C-peptide in response to secretagogues and expressed markers of pancreatic β-cells. **A**) The IBMX-based condition was evaluated for the following parameters. B) In vitro C-peptide secretion levels of differentiated cells in response to various insulin secretagogues at the end of stage 5. C-peptide secretion levels under treatment with secretagogues were compared with those detected under treatment with 2.5 mM glucose without secretagogues. C) Co-expression of pancreatic β-cell markers in INS- or CP-positive cells. Approximately 50% of INS- or CP-positive cells (red) co-expressed PDX1 (green), UCN3 (green), IAPP (green), and ISL-1 (green). Cells were counterstained with DAPI (blue). Left panel, PDX1, UCN3, IAPP or ISL1 staining (green); right panel, merged

images are shown. Results of the C-peptide secretion levels are presented as mean ± SEM of three independent experiments (n = 3). Student's *t*-tests were performed against the values of 2.5 mM glucose without secretagogues treatment, $^{**}p < 0.01$. Scale bar = 100 μm.

Supplementary Table S1: Real-time PCR primers

Genes	Primer sequences		Product (bp)
	Forward	Reverse	
GAPDH	CGAGATCCCTCCAAAATCAA	CATGAGTCCTTCCACGATACCAA	288
OCT3/4	GTATTCAGCCAAACGACCATC	CTGGTTCGCTTTCTCTTTCG	176
SOX17	GCTTTCATGGTGTGGGCTAAG	CAGCGCCTTCCACGACTT	108
FOXA2	CTGAGCGAGATCTACCAGTGGA	CAGTCGTTGAAGGAGAGCGAGT	104
HNF1β	ATAGCTCCAACCAGACTCACA	AGGCTGTGGATATTCGTCAA	313
HNF4α	CCAAGAGATCCATGGTGTTCAA	TTGATGTAGTCCTCCAAGCTCA	274
PDX1	CTTGGAAACCAACAACTATTCAC	ATTAAGCATTTCCCACAAACA	218
HNF6	AAATCACCATTTCCCAGCAG	AGCTTTTCCACCGAGGTTTT	192
NKX6.1	CCAAGAAGAAGCAGGACTCG	TCAACAGCTGCGTGATTTTC	126
SOX9	AAAGGCAACTCGTACCCAAATTT	AGTGGGTAATGCGCTTGGAT	63
PROX1	AAAGCAAAGCTCATGTTTTTTTATACC	GTAAAACTCACGGAAATTGCTAAACC	135
HLXB9	GCACCAGTTCAAGCTCAACA	GCCTTTTTGCTGCGTTTCCATTTC	135
CDX2	CTCCTCCCCAGCTCTTCTCT	TCTTAGCTGCCTTTGGCTTC	195
AFP	TGCCAACTCAGTGAGGACAA	TCCAACAGGCCTGAGAAATC	356
NGN3	TCGAGAGAGAGCGTGACAGA	CTACCGGCGCAAAAGAATAG	175
PAX4	CAGACTGTGGCTCCTTCCTC	GGGTGCTCATAGGGAAAACA	224
NEUROD1	CTCCTTCGTTCAGACGCTTT	GTGGAAGACATGGGAGCTGT	226
INS	CATCAGAAGAGGCCATCAAG	TCTTGGGTGTGTAGAAGAAGC	200
GCG	CAGAAGAGGTCGCCATTGTT	TGGCTAGCAGGTGATGTTGT	192
SST	CCAACCAGACGGAGAATGAT	AGGGAAGAGAGATGGGGTGT	241
PPY	TGCCCATTTACTCTGGACTC	ATCTGCTCTGGTGTGGCATT	160
AMY	ATTCGCAAGTGGAATGGAGA	GCCCAACCCAATCATTAACA	283
ISL1	ATTTCCCTATGTGTTGGTTGCG	CGTTCTTGCTGAAGCCGATG	229
MAF-A	TTCAGCAAGGAGGAGGTCAT	CGCCAGCTTCTCGTATTTCT	216
GCK	GGAGAGAAAGCGCTGAGGAC	CTGGTTTGGGGTTTGAGGTT	160
UCN3	GAGGGAAGTCCACTCTCGGG	TGTTGAGGCAGCTGAAGATGG	137
IAPP	AGGCAGATCACAAGGTCAGG	GTGCAATCTCGGCTCACTG	186
SLC30A8	TGTCCCAGAGAGAGACCAGA	CCACGACCTCTGCAATCATG	163

Supplementary Table S2: Primary antibodies for immunofluorescent staining

Antibody	Source	Product code	Dilution
Mouse anti-OCT3/4	Santa Cruz Biotechnology, Inc.	sc-5279	1:100
Rabbit anti-NANOG	ReproCELL	RCAB003P	1:100
Mouse anti-SSEA4	R&D Systems, Inc.	BAM1435	1:100
Mouse anti-TRA 1-81	Millipore	MAB4381	1:100
Rabbit anti-SOX2	Millipore	AB5603	1:100
Mouse anti-SSEA1	BioLegend	125603	1:100
Goat anti-SOX17	R&D Systems, Inc.	AF1924	1:100
Rabbit anti-HNF3β/FOXA2	Millipore	# 07-633	1:300
Goat anti-HNF4α	Santa Cruz Biotechnology, Inc.	sc-6556	1:100
Goat anti-PDX1	R&D Systems, Inc.	AF2419	1:100
Rabbit anti-HNF6	Santa Cruz Biotechnology, Inc.	sc-13050	1:100
Rabbit anti-SOX9	Millipore	AB5535	1:200
Mouse anti-NKX6.1	Developmental Studies Hybridoma Bank	F64A6B4	1:100
Mouse anti-CDX2	BioGenex	MU392-UC	1:500
Mouse anti-AFP	MONOSAN	MON 4035	1:200
Sheep anti-NGN3	R&D Systems, Inc.	AF3444	1:200
Rabbit anti-PAX4	Abcam	ab42450	1:200
Goat anti-NEUROD1	R&D Systems, Inc.	AF2746	1:100
Guinea Pig anti-INSULIN	Dako	A0564	1:500
Rabbit anti-C-PEPTIDE	Cell Signaling Technology, Inc.	#4593	1:200
Mouse anti-GCG	Sigma-Aldrich	G2654	1:300
Goat anti-SST	Santa Cruz Biotechnology, Inc.	sc-7819	1:500
Rabbit anti-SST	Dako	A0566	1:500
Rabbit anti-Pancreatic polypeptide	Dako	A0619	1:300
Mouse anti-Amylase	Santa Cruz Biotechnology, Inc.	sc-46657	1:100
Rabbit anti-UCN3	Phoenix Pharmaceuticals, Inc.	G-019-28	1:500
Goat anti-ISL1	R&D Systems, Inc.	AF1837	1:100
Rabbit anti-IAPP	Abcam	ab15125	1:200

CellPress

Cell Metabolism
Article

Methionine Metabolism Regulates Maintenance and Differentiation of Human Pluripotent Stem Cells

Nobuaki Shiraki,[1,8] Yasuko Shiraki,[2,8] Tomonori Tsuyama,[1,3] Fumiaki Obata,[4,5] Masayuki Miura,[4,5] Genta Nagae,[6] Hiroyuki Aburatani,[6] Kazuhiko Kume,[1,7] Fumio Endo,[2,*] and Shoen Kume[1,3,*]

[1]Department of Stem Cell Biology, Institute of Molecular Embryology and Genetics, Kumamoto University, Honjo 2-2-1, Kumamoto 860-0811, Japan

[2]Department of Pediatrics, Graduate School of Medical Sciences, Kumamoto University, Honjo 1-1-1, Kumamoto 860-8556, Japan

[3]Program for Leading Graduate Schools "HIGO," Kumamoto University, Honjo 2-2-1, Kumamoto 860-0811, Japan

[4]Department of Genetics, Graduate School of Pharmaceutical Sciences, The University of Tokyo, Hongo 7-3-1, Bunkyo-ku, Tokyo 113-0033, Japan

[5]CREST, Japan Science and Technology Agency, Chiyoda-ku, Tokyo 102-0075, Japan

[6]Genome Science Division, Research Center for Advanced Science and Technology, The University of Tokyo, Komaba 4-6-1, Meguro-ku, Tokyo 153-8904, Japan

[7]Department of Neuropharmacology, Graduate School of Pharmaceutical Sciences, Nagoya City University, 3-1 Tanabe-dori, Mizuho-ku, Nagoya 467-8603, Japan

[8]Co-first authors

*Correspondence: fendo@kumamoto-u.ac.jp (F.E.), skume@kumamoto-u.ac.jp (S.K.)

http://dx.doi.org/10.1016/j.cmet.2014.03.017

SUMMARY

Mouse embryonic stem cells (ESCs) and induced pluripotent stem cells (iPSCs) are in a high-flux metabolic state, with a high dependence on threonine catabolism. However, little is known regarding amino acid metabolism in human ESCs/iPSCs. We show that human ESCs/iPSCs require high amounts of methionine (Met) and express high levels of enzymes involved in Met metabolism. Met deprivation results in a rapid decrease in intracellular S-adenosylmethionine (SAM), triggering the activation of p53-p38 signaling, reducing NANOG expression, and poising human iPSC/ESCs for differentiation, follow by potentiated differentiation into all three germ layers. However, when exposed to prolonged Met deprivation, the cells undergo apoptosis. We also show that human ESCs/iPSCs have regulatory systems to maintain constant intracellular Met and SAM levels. Our findings show that SAM is a key regulator for maintaining undifferentiated pluripotent stem cells and regulating their differentiation.

INTRODUCTION

Embryonic stem cells (ESCs) and induced pluripotent stem cells (iPSCs) have an unlimited ability to replicate; they are pluripotent and can give rise to all cell types. ESCs/iPSCs possess a unique transcriptional circuit that sustains the pluripotent state. These cells are in a specific epigenetic state that is ready for rapid cell-fate decisions. Furthermore, various forms of histone methylation allow dynamic regulation of ESC/iPSC pluripotency and plasticity. ESCs/iPSCs also possess a characteristically high rate of proliferation as well as an abbreviated G1 phase. These unique molecular properties distinguish ESCs and iPSCs from somatic cells (Boheler, 2009).

These unusual features signify that ESCs/iPSCs exist in a specialized metabolic state. ESCs and iPSCs rely specifically on glycolysis (Armstrong et al., 2010; Facucho-Oliveira and St John, 2009), whereas somatic cells utilize mitochondrial oxidative phosphorylation for energy production. This metabolic requirement appears to play a causative role rather than being a consequence of pluripotency acquisition (Folmes et al., 2011). Recent reports have shown that metabolism is tightly linked to cellular signaling, and these two processes reciprocally regulate each other and modulate cell activities such as cell survival, proliferation, and stem cell function (Takubo et al., 2013; Wellen and Thompson, 2012).

Mouse ESCs are in a high-flux metabolic state, with a high dependence on threonine (Thr) catabolism (Alexander et al., 2011; Wang et al., 2009). It was recently reported that Thr metabolism regulates intracellular S-adenosylmethionine (SAM) and histone methylation such that depletion of Thr from the culture medium or knockdown of threonine dehydrogenase (*Tdh*) in mouse ESCs decreases SAM accumulation and trimethylation of histone H3 lysine 4 (H3K4me3), leading to slowed growth and increased differentiation (Shyh-Chang et al., 2013). However, in human cells, *Tdh* is expressed as a nonfunctional pseudogene. Furthermore, little is known regarding amino acid metabolism and its role in human ESCs/iPSCs. These reports highlight the importance of examining the metabolic state of human ESCs/iPSCs, which may improve our understanding of the signaling pathways regulating cell survival, pluripotency maintenance, and differentiation.

Methionine (Met) is an essential amino acid (Finkelstein, 1990). An important metabolite of Met is SAM, which is produced through an intermediate reaction catalyzed by methionine

adenosyltransferase (MAT). There are three major multimeric MAT enzymes: MATI, MATII, and MATIII (Halim et al., 1999). MATI is a tetramer and MATIII is a dimer of the protein encoded by *MAT1A*, whereas MATII is a dimer of the protein encoded by *MAT2A*. SAM is a methyl donor crucial for gene regulation (Lu and Mato, 2008). DNA methylation and protein methylation, including histone methylation, are catalyzed by methyltransferases by using SAM as a methyl donor (Goll and Bestor, 2005; Shi, 2007). S-adenosylhomocysteine (SAH) is generated as a product of transmethylation by methyltransferases such as DNA methyltransferases (DNMTs) and is then converted to homocysteine (Hcy) by SAH hydrolase (AHCY). Hcy is remethylated and converted to Met by 5-methyltetrahydrofolate-homocysteine methyltransferase (MTR), which requires folate and vitamin B12 or betaine-homocysteine methyltransferase (BHMT) as a methyl donor. Alternatively, Hcy is converted to cystathionine by cystathionine β-synthase (CBS) and then further metabolized to cysteine by cystathionase (CTH). The Met salvage pathway, in which S-methyl-5′-thioadenosine (MTA), a byproduct of polyamine biosynthesis, is enzymatically converted to Met through several enzymatic steps, is also involved in Met metabolism. However, no study yet has focused on the Met salvage pathway in human ESCs/iPSCs.

Here, we show that undifferentiated pluripotent human ESCs/iPSCs are in a high-Met metabolic state that decreased with differentiation. We examined the underlying mechanisms and measured metabolites.

RESULTS

Met Deprivation Causes Cell-Cycle Arrest and Impairment of Survival in Pluripotent Human ESCs/iPSCs

We first deprived single amino acids from the culture medium for 48 hr during culture of the undifferentiated human ESC line khES3 (Suemori et al., 2006) and the human iPSC line 201B7 (Takahashi et al., 2007), and we examined their impact on cell survival (Figure 1A). Deprivation of leucine (Leu), lysine (Lys), tryptophan (Trp), or Met resulted in inhibition of cell growth and decreased cell number (Figure 1A). Bright-field microscopy showed cell death when cells were grown in Leu-, Lys-, or Met-deprived conditions (Figure S1 available online). Met deprivation was the most effective growth inhibitor of human pluripotent stem cells; we therefore focused on Met.

When Met concentration in the media was reduced from 120 μM to 12 μM, self-renewal was reduced in both khES3 and 201B7 cells (Figure 1B). Similar results were observed with other human ESC (khES1) or iPSC (253G1) lines (Figure S1B). Time-dependent studies revealed a significant reduction in cell number (Figure 1C) and self-renewal (Figure 1D) as early as 5 hr after Met deprivation. Apoptosis significantly increased after 24 hr of Met deprivation (Figure 1E), and at 48 hr more than half of the cells were TUNEL-positive (Figure 1E). Apoptosis was also observed with Leu or Lys deprivation in khES3 cells (Figure S1C).

G0/G1 phase arrest, as well as a reduction in the cell population in S and G2/M phases, was observed following prolonged Met deprivation for 24 hr in both khES3 and 201B7 cells (Figure 1F). G0/G1 phase arrest was also observed after Leu and Lys deprivation for 48 hr (Figure S1D).

These results indicate that undifferentiated human ESCs/iPSCs require greater than 25 μM Met for maintenance and that deprivation of Met results in growth inhibition, followed by cell-cycle arrest and cell death.

Rapid Decrease in Intracellular SAM and MTA Levels and Cessation of Hcy Excretion after Met Deprivation

In mouse ESCs, Thr is essential for cell growth, and deprivation of Thr reduces intracellular SAM ($[SAM]_i$) levels (Shyh-Chang et al., 2013). To determine the intracellular level of Met ($[Met]_i$) and its metabolites in human ESCs/iPSCs cultured in complete (control) or Met-deprived conditions, we analyzed and quantified intracellular Met-cycle metabolites (Met, SAM, SAH, and MTA) and excreted Hcy in khES3 and 201B7 cells. The $[Met]_i$ level decreased 5 and 24 hr after Met deprivation (Figure 2A, Met). We observed a decrease in $[SAM]_i$ and $[MTA]_i$ at 5 hr, which increased 24 hr after Met deprivation, with $[SAM]_i$ returning to a level similar to that of the control (Figure 2A, SAM). MTA supplementation increased $[Met]_i$ in both control and Met-deprived conditions (Figure 2A, Met). This result suggests that human ESCs actively convert MTA into Met, and then into SAM, even in complete media. This preference of SAM and MTA utilization explains the early decrease in $[SAM]_i$ and $[MTA]_i$ at 5 hr after Met deprivation. Interestingly, a rapid release of intracellular Hcy into the media was observed in complete media (Figure 2B). Hcy excretion was not seen under Met deprivation conditions, which reoccurred when supplemented with MTA. We interpreted this result to indicate conversion of MTA into Met, which then entered the Met cycle with subsequent metabolization into Hcy. Decreased SAM and cessation of Hcy excretion were also observed in 201B7 cells (Figures 2C and 2D).

Expression profile analysis revealed that Met depletion triggered a marked downregulation of Met metabolic enzymes, including *DNMT3B* (Figures 2E and 2F). While *MAT2A*, which catalyzes the conversion of Met into SAM in pluripotent stem cells, significantly increased under Met deprivation, *MAT2B* expression was attenuated under Met deprivation, showing a rapid decrease and a later increase after 10 hr. It is possible that *MAT2A*/*MAT2B* upregulation may then lead to an increase in $[SAM]_i$ (Figure 2A, SAM).

SAM Is Crucial for Self-Renewal and Survival of Human ESCs/iPSCs

To examine the role of Met metabolism in self-renewal of human ESCs/iPSCs, we performed Met deprivation and rescue by supplementation with Met metabolites such as Met itself, SAM, Hcy, or MTA. In both khES3 and 201B7 cells, cell death induced by Met deprivation was rescued by supplementation with Met, SAM, Hcy, or MTA (Figure 3A). Met supplementation was the most effective, followed by SAM and MTA supplementation. Hcy supplementation showed limited rescue effects compared to Met. MTA supplementation also rescued cell depletion, confirming the conversion of MTA to Met through the salvage cycle (Figure 2).

These results suggest the importance of Met and SAM for maintaining ESC/iPSC self-renewal. To examine whether Met or SAM is essential for the maintenance of pluripotent stem cells, we performed knockdown of *MAT2A*, *MAT2B*, and spermine synthase (*SMS*) (Figures 3B and 3C). Knockdown of *MAT2A* or

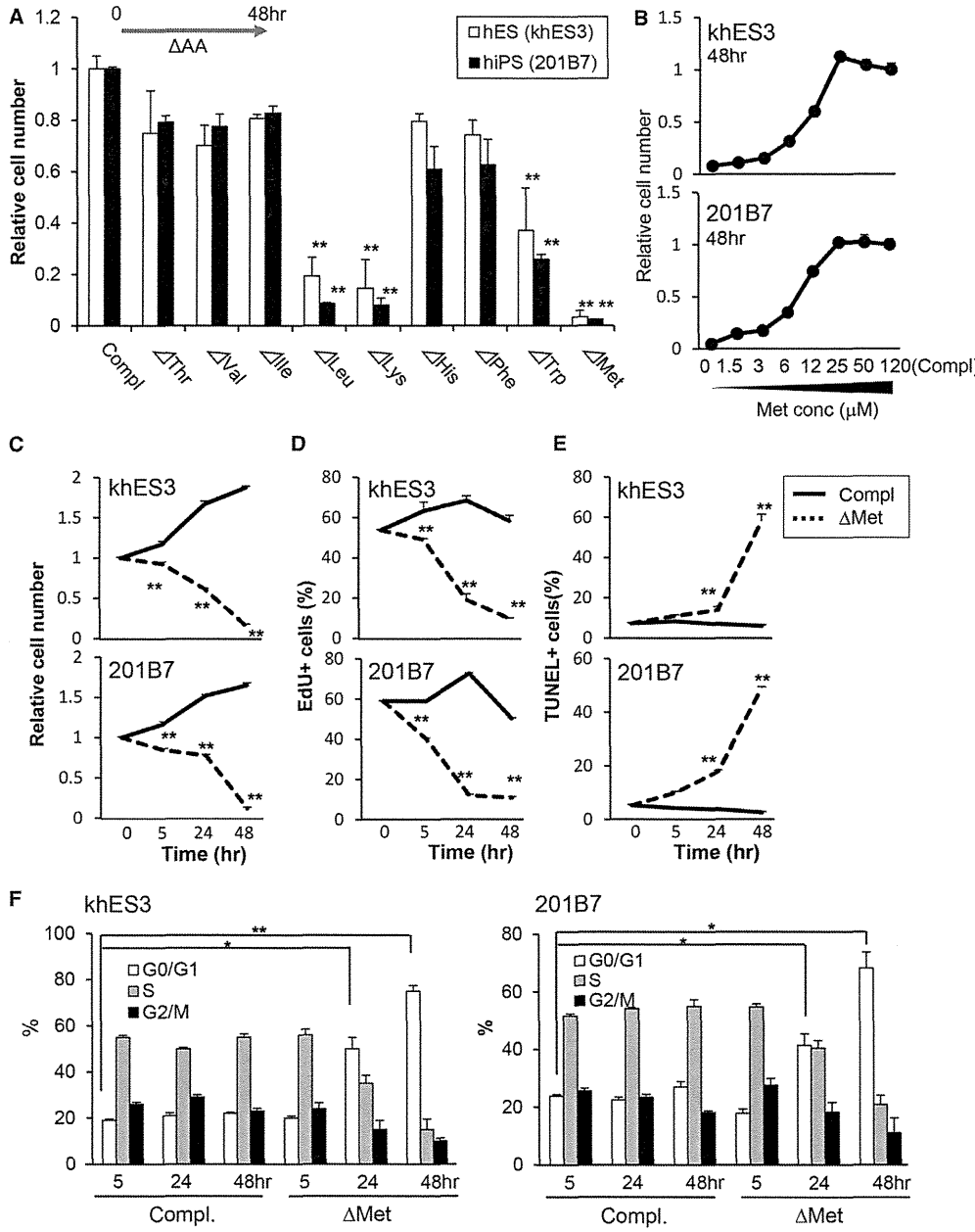

Figure 1. Impact of Met Deprivation on Undifferentiated Human ESCs/iPSCs

(A) Total number of undifferentiated khES3 (open bars) and 201B7 (black bars) cells after 48 hr amino acid deprivation.

(B–F) Shown are graded Met concentration (B) and time-dependent effects on total cell number (C), proliferation (D), apoptosis (E), and G0/G1 arrest (F). Error bars, SEM (n = 3). Significant differences were determined by Student's t test; *$p < 0.05$ and **$p < 0.01$.

MAT2B, but not *SMS*, decreased self-renewal (Figures 3B, 3C, and S2). Rescue of self-renewal by SAM addition was not affected by *SMS* knockdown (Figure 3C). The above results indicate that SAM, rather than Met itself, is essential for self-renewal and survival (Figures 3B and 3C).

Next, the effect of cycloleucine, an analog of Met that acts as a specific inhibitor of MAT (Sufrin et al., 1979), was tested. khES3 and 201B7 cells treated with increasing cycloleucine for 48 hr showed a significant decrease in cell number at 100 mM cycloleucine (Figure 3D). Cycloleucine treatment for 24 hr significantly

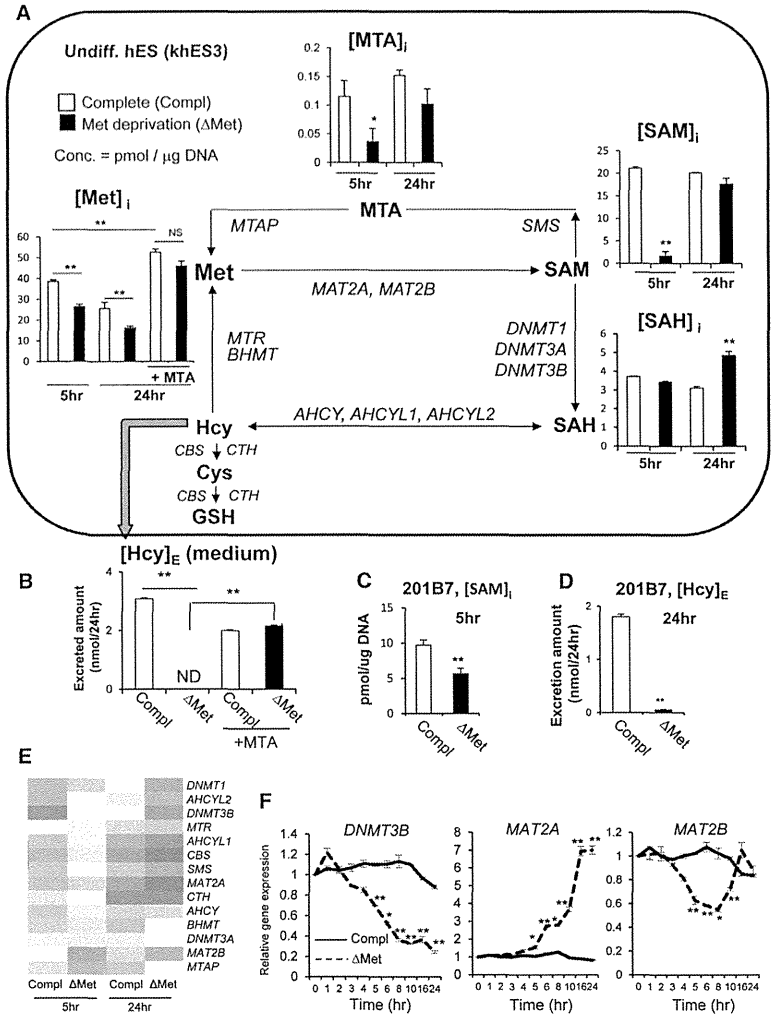

Figure 2. Measurement of Met-Cycle Metabolites

(A) Intracellular concentration of Met ($[Met]_i$), MTA ($[MTA]_i$), SAM ($[SAM]_i$), and SAH ($[SAH]_i$) in undifferentiated khES3 cells 5 and 24 hr after culture in complete (open bars) or Met-deprived (black bars) media, normalized to DNA.

(B) Hcy excretion ($[Hcy]_E$) in khES3 cells 24 hr after Met deprivation. ND, not detected.

(C) $[SAM]_i$ of undifferentiated 201B7 cells after 5 hr culture in complete (open bars) or Met-deprived (black bars) media.

(D) $[Hcy]_E$ in 201B7 cells after 24 hr culture.

(E) Expression profiles of Met-Cys metabolic enzymes in undifferentiated khES3 cells cultured in complete or Met-deprived (ΔMet) media for 5 or 24 hr.

(F) Time-dependent changes in levels of *DNMT3B*, *MAT2A*, and *MAT2B* by real-time PCR. Error bars represent SEM (n = 3). Significant differences were determined by Student's t test; NS, no significance, $^*p < 0.05$, and $^{**}p < 0.01$.

lowered $[SAM]_i$ without affecting $[Met]_i$ or $[SAH]_i$ (Figure 3E), demonstrating that SAM, but not Met, is essential for the self-renewal and survival of human ESCs/iPSCs.

Next, to examine how prolonged Met deprivation affects cell survival, we performed 5 hr and 24 hr Met deprivation studies (Figure 3F) followed by 48 hr of culture in complete or Met-deprived media in khES3 and 201B7 cells. Deprivation of Met for 5 hr was reversible, and cells proliferated after switching to complete media (Figure 3F, c). However, under prolonged (24 hr) Met deprivation, cell proliferation did not recover even when cells were switched to complete media (Figure 3F, f). This result suggests that a short Met deprivation is reversible, but prolonged Met deprivation is vital for cell survival. Considering that intracellular Met metabolite concentrations change with time (Figure 2), our results suggest that SAM may act as an early sensor. Met deprivation led to SAM reduction and decreased proliferation, and prolonged Met deprivation resulted in G0/G1 phase cell-cycle arrest (Figure 1F), which then led to apoptosis.

Met Deprivation in Undifferentiated Human ESCs/iPSCs Induced Upregulation of the p53-p38 Signaling Pathway, which Is Critical for Cell-Cycle Arrest and Apoptosis

We next attempted to identify the signaling pathway responsible for the impaired cell survival. We performed gene expression profiles of undifferentiated khES3 cells cultured in complete or Met-deprived conditions for 5 or 24 hr. Cell-cycle- and apoptosis-related genes increased by >3-fold (Figure 4A) and >2-fold (Table S1A), respectively, in the Met-deprived group compared to the complete control. Significant increases were observed in levels of p53-dependent genes involved in apoptosis, such as *ATM*, *ATR*, *MDM2*, *CDKN1A*, *FAS*, *TNFRSF10A*, and *TNFRSF10D*. Additionally, Met deprivation for 24 hr increased *CASP3* and *CASP8*, which are critical mediators of apoptosis (Figure 4A). Enrichment analysis identified signaling pathways, the expression levels of which increased by >3-fold at 5 or 24 hr Met deprivation, are shown in Table S1B.

Because transcript levels of *p53* were unchanged under Met deprivation conditions, we next examined p53 at the protein level. Total p53 protein increased within 5 hr of Met deprivation in both khES3 and 201B7 cells, detected by western blot (Figure 4B) and immunocytochemical analyses (Figure 4C). Supplementation of Met decreased the proportion of $p53^+$ cells in a concentration-dependent manner (Figure 4D). Interestingly, the increase in $p53^+$ cells was observed specifically under Met deprivation, but not under deprivation of other amino acids (Figure 4E). Moreover, p53 upregulation was completely abolished by SAM supplementation (Figure 4E, ΔMet+SAM) and triggered by cycloleucine (Figure 4F). To determine the effect of ΔMet-induced p53 on cell death in khES3 cells, we performed knockdown of *p53*

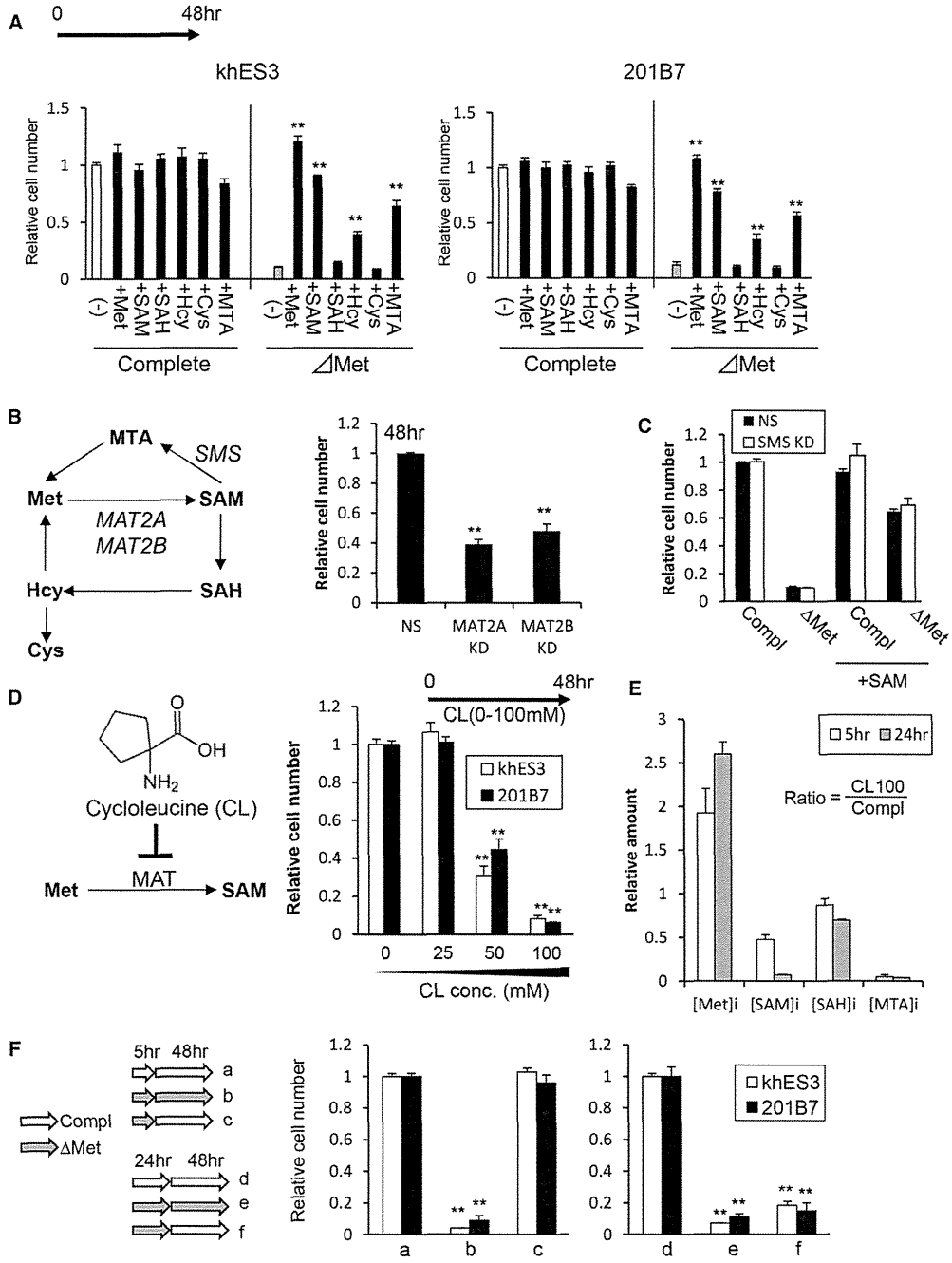

Figure 3. Met Metabolism Is Crucial for Human ESC/iPSC Proliferation

(A) Quantitative analyses of relative khES3 (left panels) and 201B7 (right panels) cell numbers after culture for 48 hr in complete or Met-deprived (ΔMet) media. Cells were supplemented with 100 μM Met, SAM, SAH, Hcy, Cys, or MTA (black bars), and cell numbers were compared with the control complete media (white bars).

(B) Relative cell numbers of nonsilenced (NS), *MAT2A*, or *MAT2B* KD khES3 cells 48 hr after knockdown.

(C) Quantitative analyses of relative cell numbers of NS or *SMS* KD khES3 cells after 48 hr culture in complete or Met-deprived (ΔMet) media. Supplementation of 100 μM SAM (+SAM).

(legend continued on next page)